Available online at www.sciencedirect.com
ScienceDirect
Journal of Sound and Vibration 304 (2007) 863–874
JOURNAL OF SOUND AND VIBRATION
www.elsevier.com/locate/jsvi

Localization of flexural waves in a disordered periodic piezoelectric beam

A-Li Chen[a], Feng-Ming Li[b], Yue-Sheng Wang[a,*]

[a]*Institute of Engineering Mechanics, School of Civil Engineering, Beijing Jiaotong University, Beijing 100044, China*
[b]*Department of Aerospace Science and Mechanics, Harbin Institute of Technology, Harbin 150001, China*

Received 3 November 2005; received in revised form 21 March 2007; accepted 23 March 2007

Abstract

Localization of bending waves in a disordered periodic piezoelectric beam is studied in this paper. The equation of the wave motion for a piezoelectric beam is derived on the assumption of an Euler–Bernoulli beam, and the harmonic solution is presented. The transfer matrix between two consecutive unit cells in the structures is obtained by using the continuity conditions. The expression of the localization factor is given by Wolf's algorithm. Numerical examples are presented and the effects of several disordered parameters on the localization factor are analyzed. The results show that piezoelectricity has obvious effects on the passbands and stopbands of the periodic piezoelectric beam. The behavior of wave propagation and localization in disordered periodic piezoelectric beams can be altered by tuning different structural parameters.

1. Introduction

Recently, periodic or nearly periodic structures are extensively used with the development of aerospace, civil engineering, rotary machines, etc. Practical periodic structures are usually different from ideal ones and may be disordered due to material defects or manufacturing errors. The perfectly periodic structures have characteristics of passbands and stopbands. While the disordered periodic structures exhibit localization of waves and vibration [1]. This behavior enables us to control the propagation of waves and vibration with particular frequencies through the structures or decrease the vibration of the important sub-structures. Furthermore, the localization characteristic has numerous potential engineering applications such as acoustic filters, vibration isolation, noise suppression and design of new transducers. On the other hand, localization breaks the regularity of the modes of periodic structures, and leads to energy storage. This may influence the structure strength and service life. So it is necessary to study the wave localization of disordered periodic structures.

Most previous studies on the problem of wave localization were devoted to disordered periodic purely elastic structures [2]. As we know, intelligent materials which can perceive the changes of outer environment and properly respond to these changes are widely applied in structures to satisfy people's requirements. Many

*Corresponding author. Fax: +86 10 51682094.
E-mail address: yswang@center.njtu.edu.cn (Y.-S. Wang).

0022-460X/$ - see front matter © 2007 Elsevier Ltd. All rights reserved.
doi:10.1016/j.jsv.2007.03.047

intelligent structures appear in the form of periodic systems [3]. Crawley and Anderson [4] developed analytical models illustrating the mechanics of Euler–Bernoulli beams with surface mounted and embedded actuators (waves propagating in these structures are flexural waves). The analytical results were verified by carrying out static experiments. As far as we know, few studies of wave localization in disordered periodic piezoelectric structures have been performed. Baz [5] investigated the problems of active vibration control and wave localization in periodic spring-mass systems controlled by piezoelectric actuators. Thorp et al. [3] studied localization phenomenon in rods with periodically shunted piezoelectric patches. And the disorder was introduced by properly tuning the shunted impedance distribution along the rod.

In the present paper, the problem of flexural wave propagation and localization in beams periodically inserted with piezoelectric materials is studied. As we known, the flexural wave is one of the most important modes propagating in beams. Use of piezoelectric materials may provide us a way to control the propagation of the flexural wave or vibration in beam-like structures. As the preliminary study, the present analysis is performed based on the assumption of an Euler–Bernoulli beam. The equation of the flexural wave motion is derived and the harmonic solution is given. The transfer matrix of the structure is deduced using the continuity conditions between two consecutive unit cells. The expression of the localization factor is presented. Numerical examples are given and the influences of the different disordered parameters on the localization factor are analyzed. The present study is relevant to the dynamic analysis and design of intelligent structures.

2. Equations of wave motion and their solutions

The uniform beam shown in Fig. 1 is built up by periodically inserting piezoelectric materials in the elastic beam which has been mentioned in Ref. [4]. The lengths of elastic and piezoelectric parts are a_1 and a_2, respectively.

As the preliminary study, we adopt the Euler–Bernoulli beam. The equation of wave motion in the elastic beam is

$$E_1 I_1 \partial^4 w_1/\partial x_1^4 + \rho_1 A \partial^2 w_1/\partial t^2 = 0 \tag{1}$$

and that in the piezoelectric beam is given by (see Appendix A for the detailed derivation)

$$E_2 I_2 \partial^4 w_2/\partial x_2^4 + \partial^2 F/\partial x_2^2 + \rho_2 A \partial^2 w_2/\partial t^2 = 0, \tag{2}$$

where w_i is the displacement component in z-direction, E_i the Young's modulus, I_i the inertial moment and ρ_i the mass density with $i = 1$ referring to the elastic beams and $i = 2$ to the piezoelectric beams. A is the area of the cross-section; $F = \int_A z e_{31} E_3 \, dA$ with e_{31} being the piezoelectric constant of the piezoelectric materials; and E_3 is the electric field which can be expressed as

$$E_3 = -\partial\phi/\partial z, \tag{3}$$

where ϕ is the electrical potential function.

Considering the equation $\nabla \cdot D = 0$ [6], where D is the electric displacement vector, we can get

$$e_{15} \partial^2 w_2/\partial x_2^2 - \varepsilon_{11} \partial^2 \phi/\partial x_2^2 = 0. \tag{4}$$

As in Ref. [7], assume that ϕ is linearly distributed in the cross-section and given by

$$\phi = (1 + az)\varphi(x_2, t), \tag{5}$$

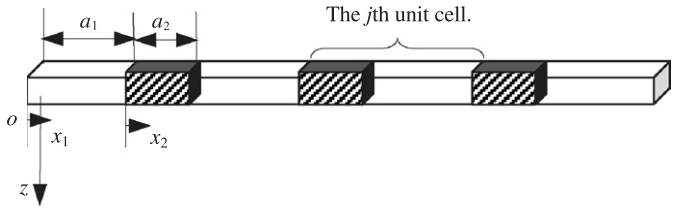

Fig. 1. Schematic diagram of a beam periodically inserted with piezoelectric materials.

where a is a parameter and will be eliminated afterwards. Substituting Eq. (5) into Eqs. (3) and (4) yields

$$E_3 = -\partial\phi/\partial z = -a\varphi(x_2, t),$$
$$e_{15}\partial^2 w_2/\partial x_2^2 - \varepsilon_{11}(1 + az)\partial^2\varphi/\partial x_2^2 = 0. \tag{6}$$

The equation of wave motion in the piezoelectric beam can be obtained from Eqs. (2) and (6):

$$E_2 I_2 \partial^4 w_2/\partial x_2^4 + E_2 I_2 b\partial^2 w_2/\partial x_2^2 + \rho_2 A\partial^2 w_2/\partial t^2 = 0, \tag{7}$$

where

$$b = -\frac{e_{31}e_{15}A}{\varepsilon_{11}E_2 I_2}$$

in which e_{15} and ε_{11} are the piezoelectric constant and dielectric constant, respectively. We look for the harmonic solution of the form

$$w_i(x_i, t) = W_i(x_i)\exp(-\mathrm{i}\omega t) \quad (i = 1, 2), \tag{8}$$

where $\mathrm{i} = \sqrt{-1}$; ω and W_i are the circular frequency and the amplitude of the displacements, respectively.

Substitution of Eq. (8) into Eqs. (1) and (7) leads to

$$\mathrm{d}^4 W_1/\mathrm{d}x_1^4 - k_1^2 W_1 = 0, \quad \mathrm{d}^4 W_2/\mathrm{d}x_2^4 + b\mathrm{d}^2 W_2/\mathrm{d}x_2^2 - k_2^2 W_2 = 0, \tag{9}$$

where

$$k_i^2 = \frac{\rho_i A\omega^2}{E_i I_i} \quad (i = 1, 2).$$

Then the equations of wave motion in elastic and piezoelectric beams can be obtained by solving Eq. (9). The solutions may be written in the following forms:

$$W_1 = A_1\cosh(\beta_1 x_1) + A_2\sinh(\beta_1 x_1) + A_3\cos(\beta_1 x_1) + A_4\sin(\beta_1 x_1), \tag{10}$$

$$W_2 = B_1\cosh(\beta_2 x_2) + B_2\sinh(\beta_2 x_2) + B_3\cos(\beta_3 x_2) + B_4\sin(\beta_3 x_2), \tag{11}$$

where

$$\beta_1 = \sqrt{k_1}, \quad \beta_2 = \sqrt{\sqrt{k_2^2 + b^2/4} - b/2} \quad \beta_3 = \sqrt{\sqrt{k_2^2 + b^2/4} + b/2};$$

and A_k and B_k ($k = 1,2,3,4$) are the unknown coefficients to be determined by the boundary conditions.

It will be convenient to cast Eqs. (10) and (11) into dimensionless forms by introducing the dimensionless local coordinates, $\xi_i = x_i/a_0$, where a_0 is the mean value of the lengths of the piezoelectric beams for the disordered systems (for the perfectly periodic system, $a_2 \equiv a_0$). Then the dimensionless forms of Eqs. (10) and (11) are given by

$$W_1 = A_1\cosh(p_1\xi_1) + A_2\sinh(p_1\xi_1) + A_3\cos(p_1\xi_1) + A_4\sin(p_1\xi_1), \tag{12}$$

$$W_2 = B_1\cosh(p_2\xi_2) + B_2\sinh(p_2\xi_2) + B_3\cos(p_3\xi_2) + B_4\sin(p_3\xi_2), \tag{13}$$

where $p_j = \beta_j a_0$ ($j = 1,2,3$); and $p_1 = \beta_1 a_0 = \sqrt{\varpi}$ with $\varpi = \omega/\sqrt{EI/\rho A a_0^4}$ being the dimensionless circular frequency.

3. Transfer matrix

Suppose that the structure shown in Fig. 1 consists of n unit cells. Each unit cell includes two sub-cells, namely, the elastic parts (sub-cell 1) and piezoelectric parts (sub-cell 2). The boundary conditions at the left

and right sides of the two sub-cells in the jth unit cell are written as

$$
\begin{aligned}
&W_{iL}^{(j)} = W_i^{(j)}(0), \quad W_{iR}^{(j)} = W_i^{(j)}(\zeta_i^{(j)}),\\
&\theta_{iL}^{(j)} = \theta_i^{(j)}(0), \quad \theta_{iR}^{(j)} = \theta_i^{(j)}(\zeta_i^{(j)}),\\
&m_{iL}^{(j)} = -\frac{E_i I_i}{a_0^2}\frac{\mathrm{d}^2 W_i^{(j)}}{\mathrm{d}\xi_i^2}(0), \quad m_{iR}^{(j)} = \frac{E_i I_i}{a_0^3}\frac{\mathrm{d}^2 W_i^{(j)}}{\mathrm{d}\xi_i^2}(\zeta_i^{(j)}),\\
&V_{iL}^{(j)} = \frac{E_i I_i}{a_0^3}\frac{\mathrm{d}^3 W_i^{(j)}}{\mathrm{d}\xi_i^3}(0), \quad V_{iR}^{(j)} = \frac{E_i I_i}{a_0^3}\frac{d^3 W_i^{(j)}}{d\xi_i^3}(\zeta_i^{(j)}),
\end{aligned}
\tag{14}
$$

where $i = 1, 2$; $j = 1, 2, \ldots, n$; $\zeta_i = a_i/a_0$ are the dimensionless lengths of the elastic and piezoelectric parts, respectively; θ_i, m_i and V_i represent the rotating angle, moment and shear force of the cross-section, respectively; and the subscripts L and R denote the left and right sides. We introduce the dimensionless moments and shear forces as follows:

$$
\begin{aligned}
&\bar{m}_{iL}^{(j)} = \frac{a_0^2}{E_i I_i} m_{iL}^{(j)}, \quad \bar{m}_{iR}^{(j)} = \frac{a_0^2}{E_i I_i} m_{iR}^{(j)},\\
&\bar{V}_{iL}^{(j)} = \frac{a_0^3}{E_i I_i} V_{iL}^{(j)}, \quad \bar{V}_{iR}^{(j)} = \frac{a_0^3}{E_i I_i} V_{iR}^{(j)}.
\end{aligned}
\tag{15}
$$

Substituting Eqs. (12) and (13) into Eqs. (14) and (15) yields

$$
\mathbf{v}_{iR}^{(j)} = \mathbf{T}_i' \mathbf{v}_{iL}^{(j)} \quad (i = 1, 2),
\tag{16}
$$

where $\mathbf{v}_{iL}^{(j)} = \{W_{iL}^{(j)}, \theta_{iL}^{(j)}, \bar{m}_{iL}^{(j)}, \bar{V}_{iL}^{(j)}\}^T$ and $\mathbf{v}_{iR}^{(j)} = \{W_{iR}^{(j)}, \theta_{iR}^{(j)}, -\bar{m}_{iR}^{(j)}, \bar{V}_{iR}^{(j)}\}^T$ are the state vectors at the left and right sides of the two sub-cells in the jth unit cell. The minus sign of $\bar{m}_{iR}^{(j)}$ is necessary when considering the direction of the moments at the two sides. $\mathbf{T}_i'$ are 4×4 transfer matrices of the two sub-cells which will be determined next. $\mathbf{v}_{iL}^{(j)}$ and $\mathbf{v}_{iR}^{(j)}$ may be rewritten as

$$
\mathbf{v}_{1L}^{(j)} = \begin{bmatrix} W_{1L}^{(j)} \\ \theta_{1L}^{(j)} \\ \bar{m}_{1L}^{(j)} \\ \bar{V}_{1L}^{(j)} \end{bmatrix} = \mathbf{P}_1 \begin{Bmatrix} A_1 \\ A_2 \\ A_3 \\ A_4 \end{Bmatrix}, \quad \mathbf{v}_{1R}^{(j)} = \begin{bmatrix} W_{1R}^{(j)} \\ \theta_{1R}^{(j)} \\ -\bar{m}_{1R}^{(j)} \\ \bar{V}_{1R}^{(j)} \end{bmatrix} = \mathbf{P}_1' \begin{Bmatrix} A_1 \\ A_2 \\ A_3 \\ A_4 \end{Bmatrix},
\tag{17}
$$

where the elements of $\mathbf{P}_1$ are $P_{11}^1 = 1$, $P_{13}^1 = 1$, $P_{22}^1 = p_1$, $P_{24}^1 = p_1$, $P_{31}^1 = -p_1^2$, $P_{33}^1 = p_1^2$, $P_{42}^1 = p_1^3$, $P_{44}^1 = -p_1^3$ with the others being zero; the matrix $\mathbf{P}_1'$ can be written as

$$
\mathbf{P}_1' = \begin{bmatrix}
\cosh(p_1\zeta_1^{(j)}) & \sinh(p_1\zeta_1^{(j)}) & \cos(p_1\zeta_1^{(j)}) & \sin(p_1\zeta_1^{(j)}) \\
p_1 \sinh(p_1\zeta_1^{(j)}) & p_1 \cosh(p_1\zeta_1^{(j)}) & -p_1 \sin(p_1\zeta_1^{(j)}) & p_1 \cos(p_1\zeta_1^{(j)}) \\
-p_1^2 \cosh(p_1\zeta_1^{(j)}) & -p_1^2 \sinh(p_1\zeta_1^{(j)}) & p_1^2 \cos(p_1\zeta_1^{(j)}) & p_1^2 \sin(p_1\zeta_1^{(j)}) \\
p_1^3 \sinh(p_1\zeta_1^{(j)}) & p_1^3 \cosh(p_1\zeta_1^{(j)}) & p_1^3 \sin(p_1\zeta_1^{(j)}) & -p_1^3 \cos(p_1\zeta_1^{(j)})
\end{bmatrix}.
$$

By means of Eqs. (16) and (17), the transfer matrix $\mathbf{T}_1'$ in sub-cell 1 can be written as

$$
\mathbf{T}_1' = \mathbf{P}_1' \mathbf{P}_1^{-1}.
\tag{18}
$$

Similarly, we get the transfer matrix $\mathbf{T}_2'$ in sub-cell 2:

$$
\mathbf{T}_2' = \mathbf{T}_2' \mathbf{P}_2^{-1},
\tag{19}
$$

in which the elements of $\mathbf{P}_2$ are $P_{11}^2=1$, $P_{13}^2=1$, $P_{22}^2=p_2$, $P_{24}^2=p_3$, $P_{31}^2=-p_2^2$, $P_{33}^2=p_3^2$, $P_{42}^2=p_2^3$, $P_{44}^2=-p_3^3$ with the others being zero; the matrix $\mathbf{P}_2'$ can be written as

$$\mathbf{P}_2'=\begin{bmatrix} \cosh(p_2\zeta_2^{(j)}) & \sinh(p_2\zeta_2^{(j)}) & \cos(p_3\zeta_2^{(j)}) & \sin(p_3\zeta_2^{(j)}) \\ p_2\sinh(p_2\zeta_2^{(j)}) & p_2\cosh(p_2\zeta_2^{(j)}) & -p_3\sin(p_3\zeta_2^{(j)}) & p_3\cos(p_3\zeta_2^{(j)}) \\ -p_2^2\cosh(p_2\zeta_2^{(j)}) & -p_2^2\sinh(p_2\zeta_2^{(j)}) & p_3^2\cos(p_3\zeta_2^{(j)}) & p_3^2\sin(p_3\zeta_2^{(j)}) \\ p_2^3\sinh(p_2\zeta_2^{(j)}) & p_2^3\cosh(p_2\zeta_2^{(j)}) & p_3^3\sin(p_3\zeta_2^{(j)}) & -p_3^3\cos(p_3\zeta_2^{(j)}) \end{bmatrix}$$

Considering the relations of $\mathbf{v}_{1L}^{(j+1)}=\mathbf{W}_1\mathbf{v}_{2R}^{(j)}$, $\mathbf{v}_{2R}^{(j)}=\mathbf{T}_2'\mathbf{v}_{2L}^{(j)}$, $\mathbf{v}_{2L}^{(j)}=\mathbf{W}_2\mathbf{v}_{1R}^{(j)}$ and $\mathbf{v}_{1L}^{(j)}=\mathbf{T}_2'\mathbf{v}_{1L}^{(j)}$, the following equation can be obtained:

$$\mathbf{v}_{1L}^{(j+1)}=\mathbf{W}_1\mathbf{T}_2'\mathbf{W}_2\mathbf{T}_1'\mathbf{v}_{1L}^{(j)}, \tag{20}$$

where the elements of the matrix $\mathbf{W}_1$ are $W_{11}^1=1$, $W_{22}^1=1$, $W_{33}^1=E_2/E_1$ and $W_{44}^1=E_2/E_1$; and those of the matrix $\mathbf{W}_2$ are $W_{11}^2=1$, $W_{22}^2=1$, $W_{33}^2=E_1/E_2$ and $W_{44}^2=E_1/E_2$ with the other elements in matrix $\mathbf{W}_1$ and $\mathbf{W}_2$ being zero.

Eq. (20) shows that the transfer matrix $\mathbf{T}_j$ between the two consecutive unit cells has the following form:

$$\mathbf{T}_j=\mathbf{W}_1\mathbf{T}_2'\mathbf{W}_2\mathbf{T}_1'. \tag{21}$$

4. Lyapunov exponents and localization factor

The Lyapunov exponent is defined as the average exponential rate of convergence or divergence between two neighboring phase orbits in the phase space and is considered as a measure of chaoticity [8]. When we study the wave propagation and localization of periodic structures, using the conception of Lyapunov exponent offers a measuring index of the attenuation degree of the wave amplitudes. Localization factor, a similar concept applied to characterize the spatial evolution of a nearly periodic system, characterizes the average exponential rate of growth or decay of the wave amplitudes [9].

According to the symmetry of periodic structures, it can be proved that Lyapunov exponents occur in pairs [10]. If the dimension of the transfer matrices is $2m\times 2m$, then there are m pairs of Lyapunov exponents having the following property:

$$\gamma_1\geqslant\gamma_2\geqslant\cdots\geqslant\gamma_m\geqslant\gamma_{m+1}(=-\gamma_m)\geqslant\gamma_{m+2}(=-\gamma_{m-1})\geqslant\cdots\geqslant\gamma_{2m}(=-\gamma_1), \tag{22}$$

The smallest positive Lyapunov exponent γ_m is defined as the localization factor because γ_m represents the wave which has potentially the least amount of decay and propagates longer distance than other waves. So γ_m describes the most important decay characters of elastic waves in disordered periodic structures.

The localization factor of the system is given by Wolf's algorithm [8]:

$$\gamma_m=\lim_{n\to\infty}\frac{1}{n}\sum_{j=1}^{n}\ln\left\|\hat{\mathbf{v}}_{2R,m}^{(j)}\right\|, \tag{23}$$

where the vector $\hat{\mathbf{v}}_{2R,m}^{(j)}$ is defined in what follows.

Assume that the dimension of the transfer matrices is $2m\times 2m$. In order to calculate the mth Lyapunov exponent, m orthogonal unit vectors of $2m$ dimension, $\mathbf{u}_1^{(0)},\mathbf{u}_2^{(0)},\ldots,\mathbf{u}_m^{(0)}$, are chosen as the initial state vectors. Eq. (20) is used to calculate the state vectors iteratively. At the kth iteration,

$$\mathbf{v}_{2R,k}^{(j)}=\mathbf{T}_j\mathbf{u}_k^{(j-1)}\quad(j=1,2,\ldots,n;\ \ k=1,2,\ldots,m), \tag{24}$$

where $\mathbf{u}_k^{(j-1)}$ are orthogonal unit vectors, while the vectors $\mathbf{v}_{2R,k}^{(j)}$ $(k=1,2,\ldots,m)$ are usually not orthogonal. The Gram–Schmidt orthonormalization procedure [10] is used to produce m orthogonal unit vectors

$$\begin{aligned}
&\hat{\mathbf{v}}_{2R,1}^{(j)} = \mathbf{v}_{2R,1}^{(j)}, \quad \mathbf{u}_1^{(j)} = \frac{\hat{\mathbf{v}}_{2R,1}^{(j)}}{\left\|\hat{\mathbf{v}}_{2R,1}^{(j)}\right\|},\\
&\hat{\mathbf{v}}_{2R,2}^{(j)} = \mathbf{v}_{2R,2}^{(j)} - (\mathbf{v}_{2R,2}^{(j)}, \mathbf{u}_1^{(j)})\mathbf{u}_1^{(j)}, \quad \mathbf{u}_2^{(j)} = \frac{\hat{\mathbf{v}}_{2R,2}^{(j)}}{\left\|\mathbf{v}_{2R,2}^{(j)}\right\|},\\
&\qquad\qquad \vdots\\
&\hat{\mathbf{v}}_{2R,m}^{(j)} = \mathbf{v}_{2R,m}^{(j)} - (\mathbf{v}_{2R,m}^{(j)}, \mathbf{u}_{m-1}^{(j)})\mathbf{u}_{m-1}^{(j)} - \cdots - (\mathbf{v}_{2R,m}^{(j)}, \mathbf{u}_1^{(j)})\mathbf{u}_1^{(j)}, \quad \mathbf{u}_m^{(j)} = \frac{\hat{\mathbf{v}}_{2R,m}^{(j)}}{\left\|\hat{\mathbf{v}}_{2R,m}^{(j)}\right\|},
\end{aligned} \tag{25}$$

where $(\cdot,\cdot)$ denotes the dot product.

In this paper $m=2$, so the smallest positive Lyapunov exponent γ_2 is the localization factor. After the localization factor is calculated, one can find that the wave amplitude attenuates in the form of $\mathbf{e}^{-\gamma_2}$ and the form of energy attenuation is $\mathbf{e}^{-2\gamma_2}$ when the wave propagates between two consecutive cells. For the waves propagating though the whole structure, the amplitude and energy attenuation coefficients are $\mathbf{e}^{-n\gamma_2}$ and $\mathbf{e}^{-2n\gamma_2}$.

5. Numerical examples and discussion

In numerical computation, $p_1=\sqrt{\varpi}$ is considered as an independent variable to analyze the effects of different disordered parameters on the localization factor. Four disordered parameters are considered, the length a_1 of the elastic beams, the length a_2 of the piezoelectric beams, the Young's module E_2 and the piezoelectric coefficient e_{31}. For convenience, let L denote a_1, a_2, E_2 and e_{31}. L is assumed to be a uniformly distributed random variable with the mean value L_0 and variation coefficient δ. So L is a random number at the interval

$$L \in [L_0(1-\sqrt{3}\delta), L_0(1+\sqrt{3}\delta)]. \tag{26}$$

Introduce a standard uniformly distributed random variable, $t\in(0,1)$. Then L can be expressed as

$$L = L_0[1+\sqrt{3}\delta(2t-1)]. \tag{27}$$

5.1. Localization factors of the ordered beam with different piezoelectric constant

Consider the beam consisting of the piezoelectric material, PZT-5 H, and the elastic material, aluminum, alternately. Assume that $a_1=2a_0$ and $a_2=a_0$, then we have $\zeta_1=a_1/a_0=2.0$ and $\zeta_2=a_2/a_0=1.0$. Fig. 2 illustrates the localization factors of the ordered beam with different piezoelectric constant e_{31}. According to the definition of the localization factors, when localization factors are equal to zero then the corresponding frequency intervals are known as passbands. When localization factors are positive, then the intervals are known as band gaps or stopbands. The results show distinguished difference between the purely elastic periodic beam ($e_{31}=0$) and the piezoelectric one ($e_{31}\neq0$). Meanwhile, it can be seen that the localization factors increase significantly with the decrease of the values of e_{31}. In one word, piezoelectricity has obvious effects on the passbands and stopbands of the periodic piezoelectric beam.

5.2. Disorder in the length of the elastic parts

Assume that $a_1=2[1+\sqrt{3}\delta(2t-1)]a_0$ and $a_2=a_0$, then we have $\zeta_1=a_1/a_0=2[1+\sqrt{3}\delta(2t-1)]$ and $\zeta_2=a_2/a_0=1$. For the Al/PZT-5H system the variation of the localization factor with $\sqrt{\varpi}$ for some selected

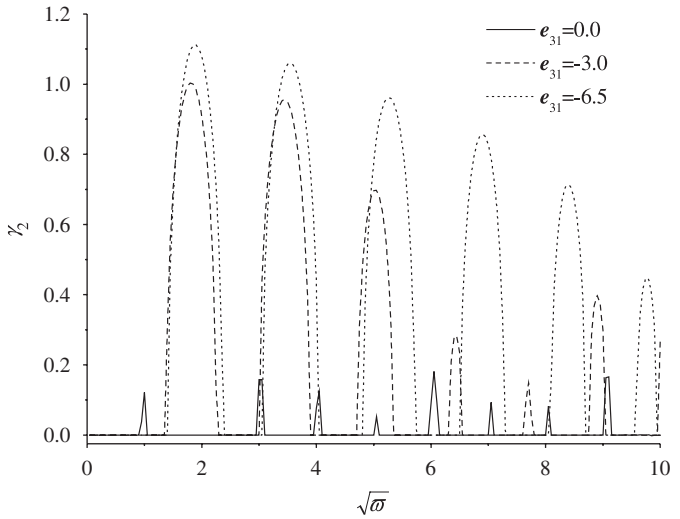

Fig. 2. Influence of the piezoelectric constant e_{31} on the localization factors.

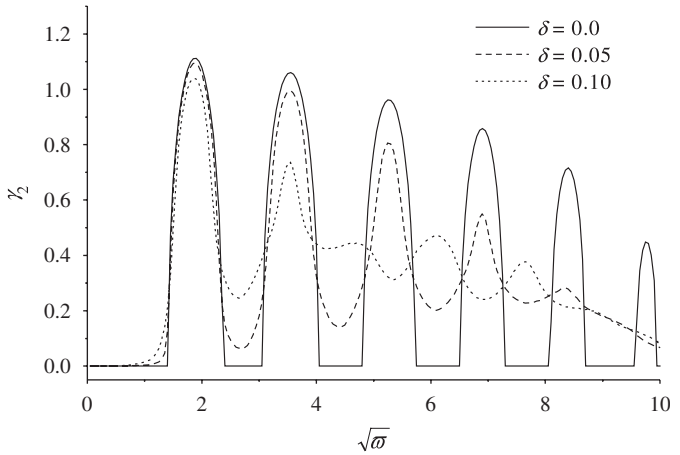

Fig. 3. Influence of the variation coefficient on the localization factors.

values of δ is shown in Fig. 3. We can see that for $\delta = 0$ the localization factors are positive in the frequency interval of $\sqrt{\varpi} \in (3.1, 4.1)$ and this interval is known as a stopband, while in the interval of $\sqrt{\varpi} \in (4.1, 4.8)$ the localization factors are zero and this interval is called a passband. However in the interval of $\sqrt{\varpi} \in (4.1, 4.8)$ the localization factors are positive in the case of $\delta \neq 0$. This is the so-called wave localization phenomenon. Similar results can be seen in the interval of $\sqrt{\varpi} \in (5.8, 6.5)$. It is shown that, with the increase of the variation coefficient, δ, the localization factors are no longer zero in the passbands and the degree of localization will increase.

Suppose that the elastic material is aluminum and the piezoelectric material is PZT-4, PZT-5H and P-7, respectively. The variation of the localization factors with different materials is shown in Fig. 4 for $\delta = 0.05$. It is seen that the localization behavior is similar for various materials except in higher frequencies. For instance, the localization factors for the piezoelectric material of PZT-4 are larger than those for other two piezoelectric materials PZT-5H and P-7, especially in higher frequencies.

5.3. Disorder in the length of the piezoelectric parts

Assume that $a_1 = 2a_0$ and $a_2 = [1 + \sqrt{3}\delta(2t - 1)]a_0$, then we can have $\zeta_1 = a_1/a_0 = 2$ and $\zeta_2 = a_2/a_0 = 1 + \sqrt{3}\delta(2t - 1)$. For the Al/PZT-5H system, the variation of the localization factors with $\sqrt{\varpi}$

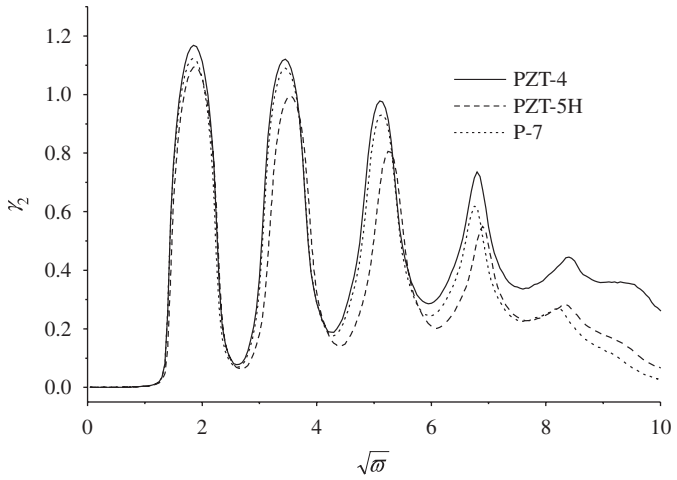

Fig. 4. Localization factors versus frequency for different piezoelectric materials.

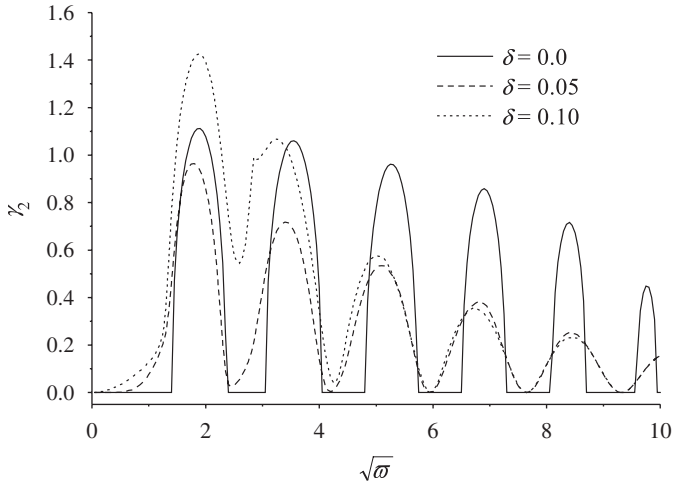

Fig. 5. Influence of the variation coefficient on the localization factors.

for some selected values of δ is shown in Fig. 5. We find the similar phenomenon as shown in Fig. 3. For example, at the interval of $\sqrt{\varpi} \in (4.0, 4.8)$, the localization factors are zero for the case of $\delta = 0$ and this frequency interval is a passband. But in this passband the localization factors are positive for the case of $\delta \neq 0$, i.e., localization phenomenon appears. Comparing Fig. 3 with Fig. 5 we can find that the localization induced by the disorder in length (a_2) of the piezoelectric beams (see Fig. 5) is more obvious than that induced by the disorder in length (a_1) of the elastic beams (see Fig. 3) in lower frequencies and vise versa in higher frequencies.

Fig. 6 shows the variation of the localization factors with the frequency for different piezoelectric materials Al/PZT-4, Al/PZT-5H and Al/P-7. Obvious difference is observed between Al/PZT-4 system and the other two systems which exhibit little difference especially in the high frequencies.

5.4. Disorder in Young's modulus of the piezoelectric parts

Consider a beam which is formed by aluminum and PZT-5H alternately. We take $a_1 = 2a_0$ and $a_2 = a_0$ or equivalently $\zeta_1 = a_1/a_0 = 2$ and $\zeta_2 = a_2/a_0 = 1$, and assume the disordered parameter $E_2 = [1 + \sqrt{3}\delta(2t - 1)]E_{20}$ with E_{20} being the mean Young's modulus of the sub-cell 2. The localization factors for some selected

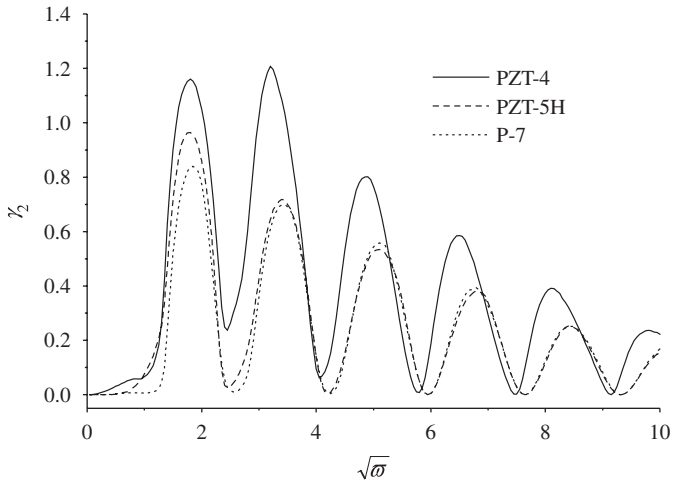

Fig. 6. Localization factors versus frequency for different piezoelectric materials.

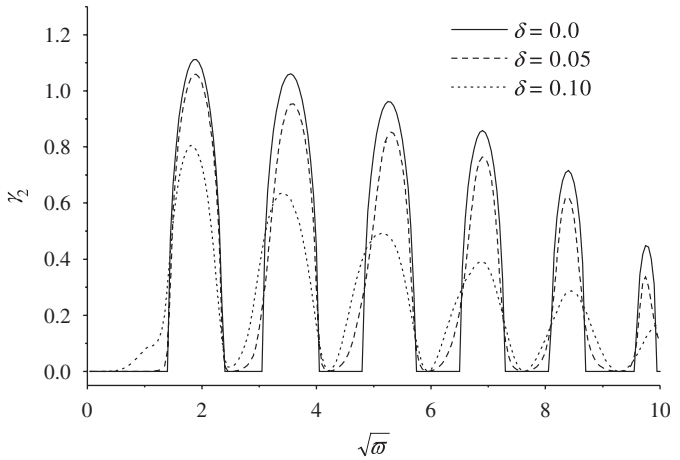

Fig. 7. Influence of the variation coefficient on the localization factors.

values of the variation coefficient are shown in Fig. 7. Localization phenomenon appears for $\delta \neq 0$. It is seen that for lower frequencies the values of localization factors in the stopbands decrease with the increase of the variation coefficient. Compared with Fig. 5, the localization behavior induced by the disorder in Young's modulus is different from that induced by the disorder in length especially in lower frequencies.

Fig. 8 illustrates the influences of the dimensionless length of the elastic parts on the localization factor for $\delta = 0$. It can be seen that ζ_1 has significant effect on the passbands and stopbands. For example, the interval $\sqrt{\varpi} \in (4.1, 4.8)$ is a passband when $\zeta_1 = 2.0$, but the corresponding interval shifts to $\sqrt{\varpi} \in (3.2, 3.8)$ when $\zeta_1 = 2.5$. Generally speaking, decrease in length of the sub-cells will move the passbands or stopbands to the higher-frequency regions.

5.5. Disorder in piezoelectric constant

Consider Al/PZT-5H system with $\zeta_1 = a_1/a_0 = 2.0$, $\zeta_2 = a_2/a_0 = 1.0$ and the disordered parameter $e_{31} = [1 + \sqrt{3}\delta(2t - 1)]e_{310}$ where e_{310} is the mean piezoelectric constant of the sub-cell 2, the influence of the variation coefficient on the localization factors are shown in Fig. 9. The trends of the curves in Fig. 9 are almost the same as those shown in Fig. 7 which means that disorder in Young's module E_2 or in e_{31} has similar effects on the wave propagation and localization of the beam.

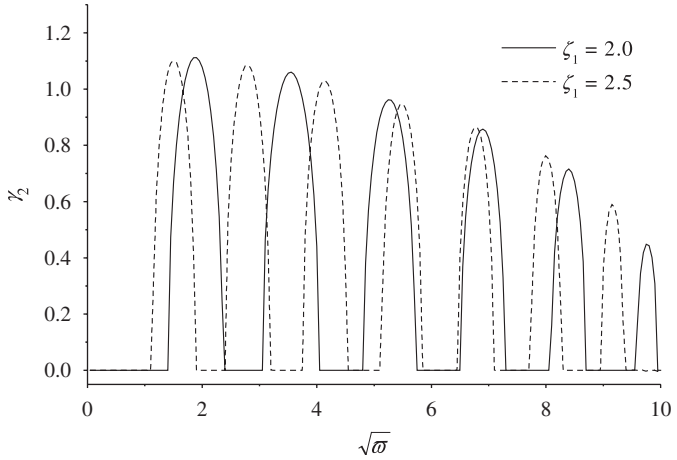

Fig. 8. Influence of the dimensionless length of the elastic parts on the localization factors.

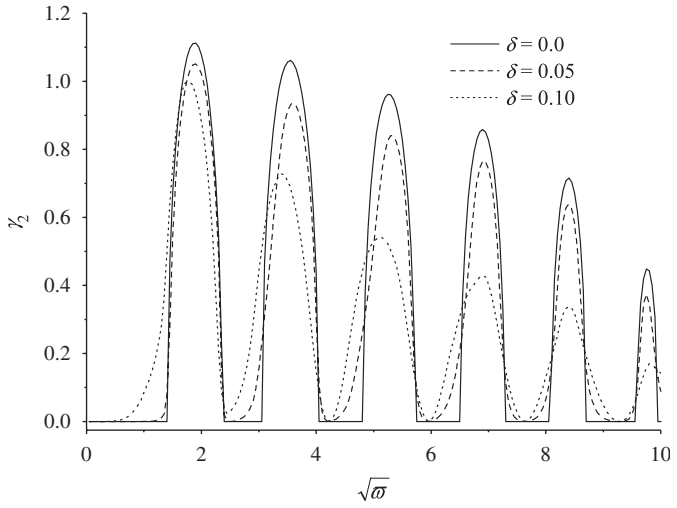

Fig. 9. Influence of the variation coefficient on the localization factors.

6. Conclusions

In this paper, the problem of wave propagation and localization in a randomly disordered periodic piezoelectric beam is studied. The following conclusions can be drawn:

(i) Turned periodic structures have the properties of the frequency passbands and stopbands and the localization phenomenon can occur when the structures are mistuned. The degree of the wave localization and behavior of passbands/stopbands can be changed by tuning the material or geometrical properties of the structures.

(ii) Piezoelectricity has obvious effects on the passbands and stopbands of the periodic piezoelectric beam. And the value of the piezoelectric constant has influence on the degree of the wave localization.

(iii) For different disordered parameters, the localization behaviors are different. The localization induced by the disorder in length (a_2) of the piezoelectric beams is more obvious than that induced by the disorder in length (a_1) of the elastic beams in lower frequencies and vise versa in higher frequencies. And the localization behavior induced by the disorder in Young's modulus is different from that induced by the disorder in length especially in lower frequencies.

(iv) The dimensionless lengths of the elastic parts have considerable influences on the wave propagation and localization behaviors of the structures. Disorder in Young's module (E_2) or in the piezoelectric constant (e_{31}) has similar effects on the wave propagation and localization of the piezoelectric beam.

According to the above conclusions, we can design different disordered periodic structures with different wave propagation and localization behaviors by properly adjusting the values of the structure constants. It should be noted again that in this paper the beam is modeled as an Euler–Bernoulli beam without considering the shearing deformation. Thus the analysis presented in this paper can only be accepted as a first rough one. To obtain more accurate results, it makes more sense to model the beam as a Timoshenko beam instead of an Euler–Bernoulli beam and this will be considered in our further studies.

Acknowledgments

Support by the National Natural Science Foundation of China under Grant 10632020 and 10672017 is grateful acknowledged.

Appendix A

Derivation of Eq. (2) is presented here. The considered material is a piezoelectric solid. For simplification the subscripts in all formulae are left out.

According to the assumption of the Euler–Bernoulli beam (see Fig. 1), we know that the longitudinal strain at coordinate (x, z) of the cross-section of the material is

$$\varepsilon = \frac{z\,\mathrm{d}\theta}{\mathrm{d}x} \tag{A.1}$$

and the curvature of the neutral layer is

$$\frac{1}{\rho} = \left|\frac{\mathrm{d}\theta}{\mathrm{d}x}\right|, \tag{A.2}$$

where ρ is the radius of the curvature and is non-negative. From Eqs. (A.1) and (A.2) we get

$$\varepsilon = \frac{z}{\rho}. \tag{A.3}$$

The constitutive equation of the piezoelectric beam is [5]

$$\sigma = E\varepsilon - e_{31}E_3. \tag{A.4}$$

Consider the dynamic equilibrium equations

$$M_y = \int_A z\sigma\,\mathrm{dA} = M, \tag{A.5}$$

where M is the moment of the cross-section. Substitution of Eqs. (A.3) and (A.4) into Eq. (A.5) yields

$$\frac{1}{\rho} = \frac{M + \int_A ze_{31}E_3\,\mathrm{dA}}{EI} \tag{A.6}$$

and the geometrical relationship is

$$\frac{1}{\rho} = \left|\frac{\mathrm{d}\theta}{\mathrm{d}s}\right| = \frac{|w''|}{(1+w'^2)^{3/2}}. \tag{A.7}$$

For general beams used in engineering, the lines of deflection are smooth. So w' is very small and can be neglected. In the coordinates shown in Fig. 1, the orientations of M and w'' are contrary. So we have the

following equation based on (A.6) and (A.7),

$$w'' = -\frac{M + \int_A ze_{31}E_3 \, dA}{EI}, \tag{A.8}$$

which can be rewritten in the form

$$M = -EIw'' - \int_A ze_{31}E_3 \, dA. \tag{A.9}$$

On the other hand, we have the following equilibrium differential equation [11]:

$$\frac{\partial^2 M}{\partial x^2} + f(x,t) = \rho A \frac{\partial^2 w}{\partial t^2}, \tag{A.10}$$

where $f(x, t)$ is the external force of the beam. For free vibration, we have

$$\frac{\partial^2 M}{\partial x^2} = \rho A \frac{\partial^2 w}{\partial t^2}. \tag{A.11}$$

Substitution of Eq. (A.9) into Eq. (A.11) yields the equation of wave motion for a piezoelectric beam in the following form:

$$EI \frac{\partial^4 w}{\partial x^4} + \frac{\partial^2}{\partial x^2}\left[\int_A ze_{31}E_3 \, dA\right] + \rho A \frac{\partial^2 w}{\partial t^2} = 0. \tag{A.12}$$

Let $F = \int_A ze_{31}E_3 \, dA$, then we get Eq. (2).

References

[1] F.M. Li, Y.S. Wang, C. Hu, W.H. Huang, Localization of elastic waves in periodic rib-stiffened rectangular plates under axial compressive load, *Journal of Sound and Vibration* 281 (2005) 261–273.
[2] F.M. Li, Y.S. Wang, W.H. Huang, C. Hu, Advances of elastic wave and vibration localization in disordered periodic structures, *Advances in Mechanics* 35 (2005) 498–512 (in Chinese).
[3] O. Thorp, M. Ruzzene, A. Baz, Attenuation and localization of wave propagation in rods with periodic shunted piezoelectric patches, *Smart Materials and Structures* 10 (2001) 979–989.
[4] E.F. Crawley, E.H. Anderson, Detailed models of piezoelectric actuation of beams, *Journal of Intelligent Material Systems and Structures* 1 (1990) 4–25.
[5] A. Baz, Active control of periodic structures, *Journal of Vibration and Acoustics* 123 (2001) 472–479.
[6] F.X. Zhang, *Modern Piezoelectricity*, Science Press, Beijing, 2001 (in Chinese).
[7] J. Wauer, Vibrations of piezoceramic rods, *Proceedings of Applied Mathematics and Mechanics* 4 (2004) 121–122.
[8] A. Wolf, J.B. Swift, H.L. Swinney, J.A. Vastano, Determining Lyapunov exponents from a time series, *Physica D* 16 (1985) 285–317.
[9] M.P. Castanier, C. Pierre, Lyapunov exponents and localization phenomena in multi-coupled nearly periodic systems, *Journal of Sound and Vibration* 183 (1995) 493–515.
[10] W.C. Xie, Buckling mode localization in rib-stiffened plates with randomly misplaced stiffeners, *Computers and Structures* 67 (1998) 175–189.
[11] A. Gani, M.J.E. Salami, R. Khan, Active vibration control of a beam with piezoelectric patches: real-time implementation with xPC target, *Control Applications, 2003 (CCA 2003)*, *Proceeding of 2003 IEEE Conference*, Vol. 1, June 2003, pp. 538–544.